JOURNAL OF THERMOPHYSICS AND HEAT TRANSFER
Vol. 6, No. 4, Oct.–Dec. 1992

Bias in Emission Absorption Measurements of Temperature and Atomic Density

Leslie E. Bauman*
Mississippi State University, Mississippi State, Mississipi 39762

Presented here is an analysis of the bias arising from two fundamental difficulties in applying emission absorption methods to large-scale combustion systems: 1) maintaining clean optical windows; and 2) maintaining the optical alignment. The impetus for the study was an anomalously large temperature measurement uncertainty for potassium D-line measurements in a coal-fired magnetohydrodynamic (MHD) flow, while no increased uncertainty was observed for the measured seed atom density. The large uncertainty can be explained by a rapid, oscillatory misalignment. This misalignment biases the measured temperature in the same manner as that for a fouled lamp-side window. Expressions for the biases for fouled optical windows are presented. Expressions are developed for the bias and uncertainty caused by a harmonic misalignment. These expressions provide a consistent explanation of the temperature results. In contrast, the robustness of a two-wavelength emission absorption method for atomic density measurements is demonstrated.

Introduction

A MULTIWAVELENGTH emission absorption instrument has been used on prototype-scale coal-fired magnetohydrodynamic (MHD) facilities for the past two years in order to determine the average temperature and average number density of neutral seed atoms.[1] Accurate measurements of temperature and seed atom density, and by inference, electron density are important for analysis of MHD channel performance, heat transfer effects, fouling of components, and seed regeneration.[2] The instrument was designed to provide line-of-sight average measurements on particle-laden flows by utilizing a two-wavelength spectroscopic method, which eliminates broadband particle effects of emission, absorption, and out-scattering and reduces error due to in-scatter.[3] The spectral measurements are made on the wings of the atomic resonance line so that the results yield values that approximate the hot core region of the flow, with a small, near constant error from a thermal boundary layer.[4,5] The primary advantage of the technique is the minimization of error caused by particle effects, which can be substantial in large-scale coal-fired flows. Comparisons show that classical, that is, single wavelength, measurements underestimate the gas temperature and overestimate the emitter atom number density, with the results sensitive to the choice of measurement wavelength. Typical test results on large-scale MHD facilities—optical path lengths of greater than 20 cm—reveal bias in single wavelength methods caused by coal ash/seed particles greater than 100 K in temperature and 100% in number density. In comparison, the reduced error and the insensitivity of the two-wavelength method to the choice of measurement wavelengths makes the method amendable for automatic measurements.[6,7]

An acceptable tradeoff to the reduced particle bias in the two-wavelength method is an increased measurement uncertainty, which for temperature is typically double that for a single wavelength measurement. On a well-controlled laboratory burner, the measurement uncertainty is on the order of 15–20 K and uncertainties larger than the instrument uncertainty have been explained by fluctuations in the flow.[8,9] However, emission absorption measurements on a recent MHD power extraction test yielded extraordinarily large temperature measurement uncertainties for a portion of the test. The analysis of the system performance on that test is the subject of this article and demonstrates the robustness of the two-wavelength technique for measurement of atomic density.

Figures 1 and 2 show, respectively, the measured gas temperature and potassium atom number density for the MHD test (89-CFC-15).[10] The facility, burning coal with vitiated air and secondary oxygen injection, has nominal input power of 50 MWt and output of 1.2 MWe. Potassium carbonate was injected to provide 1.52% potassium by weight. The supersonic linear generator is 4.35 m in length and used a diagonal electrode arrangement with a magnetic field of 2.9 T. Measurements were made at optical ports in the center of the 1.8-m subsonic diffuser test section—downstream from the MHD generator and the 1.5-m supersonic diffuser, and just upstream from a water quench ring. The optical path length through the seeded combustion products flow was 32 cm. The instrument, as configured for this test, had a resolution of about 0.3 nm FWHM, sufficient to resolve the potassium D-line wings.

Relevant test log notes are shown in Table 1. The second half of the recorded data, during which time the magnetic field was energized, seems typical for potassium emission absorption (PEAS) measurements; prior to channel operation

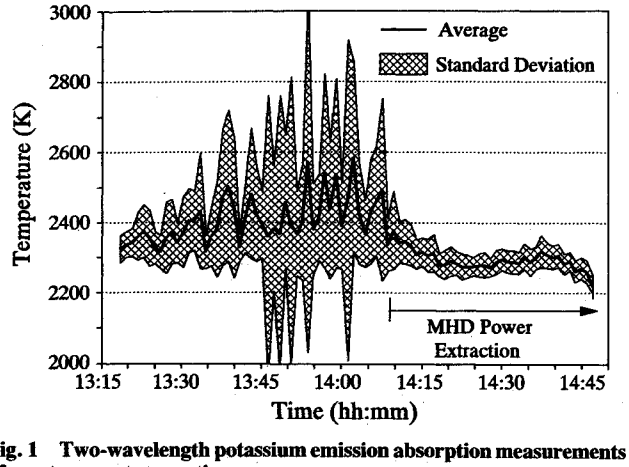

Fig. 1 Two-wavelength potassium emission absorption measurements of gas temperature vs time.

Received Sept. 5, 1990; presented as Paper 91-0212 at the AIAA 29th Aerospace Sciences Meeting, Reno, NV, Jan. 7–10, 1991; revision received Oct. 22, 1991; accepted for publication Oct. 23, 1991.

*Senior Research Scientist, Diagnostic Instrumentation and Analysis Laboratory, and Professor of Physics. Member AIAA.

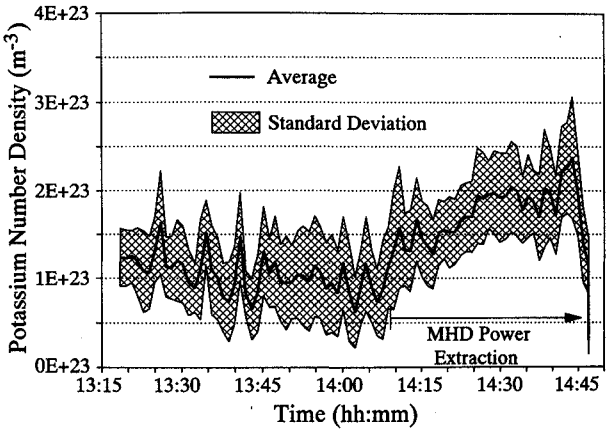

Fig. 2 Two-wavelength potassium emission absorption measurements of potassium atom number density vs time.

Table 1 Coal-fired MHD test notes

Time	Note
13:14:29	Coal-fired combustor ignition
13:18:29	Seed flow initiated
13:58:00	Invertor on-line
14:00:02	Starting magnet, gradual power up
14:15:25	Magnet at 4000 A
14:16:50	Begin increasing magnet and invertor
14:26:54	Magnet at full power (2.92 T)
14:54:00	Seed system in manual
15:10:00	Seed flow steadily dropping, trying to restore
15:15:00	Seed system in automatic

the temperature results are anomalous. In contrast, the potassium number density results seem typical throughout the measurement period. The test continued for several hours after fouling of the optical windows became too severe to continue diagnostic measurements.

Two questions arise from this test. First, what causes the extreme temperature uncertainties in the first half of the test? Second, in light of the large temperature uncertainties, are the potassium density measurements valid? The density results reveal a generally higher value during magnet operation and also a drop that occurs at the same time as the window fouling near the end of the measurements. An analysis of the effect of loss of window transmission given below implies that the seed atom density drop is real. This drop does occur before the test log indicates problems with the seed flow system.

The anomalous temperature measurement uncertainty, which disappears with extraction of power from the MHD channel, is puzzling. The raw data reveal large fluctuations in the transmitted lamp signal that disappear with power extraction, while the emission-only signal has a relatively constant signal-to-noise ratio for the entire span of measurements. This disparity cannot then be explained by a change in temperature or by number density fluctuations in the gas flow because such fluctuations would effect the emission-only signal as well. The most likely source of the uncertainty would be a rapidly fluctuating misalignment of the reference lamp beam. This misalignment could arise from vibrations of the optical mounts affixed on rails to the diffuser. The change in aerodynamic noise from the channel when power is extracted could explain the reduction in vibrations. However, we have not experienced such problems with operation of this instrument previously. Beam steering caused by pressure gradients in the flow could possibly explain the anomalous results. Velocity measurements for the same test indicated that before power is extracted, there are large recirculation regions in the diffuser that rapidly shift from one wall to the other. Velocity measurements on a subsequent test recorded alternating supersonic and subsonic velocities, indicating the presence of the shock wave in the subsonic diffuser. Presented here is an analysis of the effect on emission absorption measurements of a fluctuating misalignment using a harmonic oscillator model. This model provides a consistent explanation of the test results and reveals the robustness of the two-wavelength method for atomic density measurements.

Measurement Techniques

Consider a parallel, axisymmetric source light passing through an emitting, absorbing, and scattering medium that is a hot gas at a temperature T_g containing particles at temperature T_p. The assumptions are made of local thermodynamic equilibrium and constant properties across the flow such that

$$I_\lambda(L) = \frac{\alpha_\lambda + z\eta}{\alpha_\lambda + \eta E} B_\lambda(T_g)[1 - e^{-\tau_\lambda}] + I_\lambda(0)e^{-\tau_\lambda} + J_\lambda \quad (1)$$

where $I_\lambda(L)$ is the intensity exiting the flow of path length L, $I_\lambda(0)$ is the incident lamp intensity, α_λ is the absorption coefficient of the gas, $\tau_\lambda = (\alpha_\lambda + \eta E)L$ is the optical depth, and $B_\lambda(T_g)$ is the Planck spectral blackbody function at the temperature. The term J_λ represents the in-scattered radiation exiting the out-going boundary of the medium. Here the extinction-to-absorption ratio for the particles has been introduced as E and n is the particle absorption coefficient. The explicit dependence on the particle temperature has been removed by using the ratio $z = B_\lambda(T_p)/B_\lambda(T_g)$. The wavelength subscripts on the particle parameters have been omitted because they vary relatively slowly compared to the atomic absorption coefficient.

Although Eq. (1) was derived for isothermal flows, it is a useful approximation for boundary-layer flows. The narrower absorption linewidth of a cooler boundary layer affects significantly only the center region of the line, as evidenced in a pronounced center dip. For wavelengths outside the center dip, typically at optical depths of less than 1, the absorption coefficient and temperature are well described by averages that approach the values of the hottest region of the flow.[4,5]

One-Wavelength Temperature Determination

The classical, one-wavelength emission absorption calculation of gas temperature can be made from measurements of the signals of lamp-plus-flame, flame only, and preflame lamp, with parameters subscripted for wavelength λ_1:

$$M_1 = K_1\left[\frac{\alpha_1 + z\eta}{\alpha_1 + \eta E} B_1(T_g)[1 - e^{-\tau_1}] + J_1 + I_1(0)e^{-\tau_1}\right] \quad (2a)$$

$$M_2 = K_1\left[\frac{\alpha_1 + z\eta}{\alpha_1 + \eta E} B_1(T_g)[1 - e^{-\tau_1}] + J_1\right] \quad (2b)$$

$$M_3 = K_1 I_1(0) \quad (2c)$$

Here K_1 is the collection efficiency of the detection system, which need not be known because only ratios of signals at a single wavelength are used in the calculations. The optical depth is found from the measurements as

$$\tau_1 = \ln[M_3/(M_1 - M_2)] \quad (3)$$

Then the ratio of Planck functions at the gas and effective lamp temperature is given by

$$\Phi_1 = [M_2/(M_3 - M_1 + M_2)] \approx B_1(T_g)/I_1(0) \quad (4)$$

and the measured gas temperature is

$$T_g = (1/T_l - (\lambda_1/C_2) \ln \Phi_1)^{-1} \quad (5)$$

Two-Wavelength Temperature Determination

Similarly, Φ_2 and τ_2 can be found for a second independent wavelength on the resonance line and an approximate expression can be written for the blackbody ratio that accounts for particle out-scatter and cancels much of the particle in-scatter

$$\Phi_{1,2} \approx (\tau_1\Phi_1 - \tau_2\Phi_2)/(\tau_1 - \tau_2) \tag{6}$$

This equation is the so-called two-wavelength calculation used for these emission absorption temperature measurements. If necessary, a recursive form can also be written to account for differing Planck ratios for widely separated wavelengths.

One-Wavelength Emitter Number Density Determination

Atomic density can be determined from spectrally integrated or resolved emission absorption measurements. Because the potassium D-lines in MHD flows are very broad as well as opaque near line center, spectrally resolved measurements in the line wing are typically used to determine the atomic density. The optical depth is related to the atomic density through the wavelength dependent absorption cross section σ_λ as

$$\tau_\lambda = \alpha_\lambda L = n_K \sigma_\lambda L \tag{7}$$

A particularly simple expression can be used for determining the emitter atom number density if the absorption cross section can be modeled by a Voigt profile, which, in the line wings, has a Lorentzian shape.[5] In this case, the atomic absorption coefficient α_λ is given by

$$\alpha_\lambda \approx n_K a_2 a_\lambda / T_g^{0.5} \tag{8}$$

where n_K is the seed atom number density labeled here for potassium (K). The constant a_2 depends upon the constituents of the flow through collision effects

$$a_2 = \frac{e^2}{2m_e c^3}\left[\frac{8k}{\pi}\left(\frac{1}{m_K} + \frac{1}{m_f}\right)\right]^{0.5} n_s T_s \frac{P}{P_s} \tag{9}$$

where e is the electron charge, m_e is the electron mass, c is the speed of light, k is the Boltzmann constant, m_K is the seed atom mass, m_f is the foreign atom mass, n_s is the number density at standard temperature and pressure, T_s is the standard temperature, P is the pressure, and P_s is the standard pressure. The parameter a_λ contains the wavelength dependence as follows for a doublet line:

$$a_\lambda = \sum_{i=1}^{2} \frac{f_i \sigma_i^2}{(\lambda - \lambda_i)^2}\lambda^2\lambda_i^2 \tag{10}$$

where f_i are the oscillator strengths[11] subscripted for the two lines of the doublet, σ_i^2 are the collision cross sections,[12] and λ_i are the line center wavelengths of the doublet.

Two-Wavelength Emitter Number Density Determination

Using the previous expressions, the difference in optical depths at two wavelengths eliminates broadband contributions to the optical depth. Then number density of the seed atom, here labeled for potassium can be found as

$$n_K = (\tau_1 - \tau_2)/[(\sigma_1 - \sigma_2)L] \tag{11}$$

The far wings of the Potassium doublet have been observed to be non-Voigt under MHD conditions.[13,14] An experimental power law profile for the blue wing absorption cross section was used for the one- and two-wavelength results reported here.[15]

Window Fouling

A significant source of bias in emission absorption measurements on large-scale combustion flows is the fouling of the optical windows. Depending upon the optical port design and the flow patterns, the fouling could occur on one or both windows. Introducing t_d and t_l as the detector and lamp-side window transmissivities, respectively, Eqs. (2a), (2b), and (2c) become

$$M_1 = K_1 t_d\left[\frac{\alpha_1 + z\eta}{\alpha_1 + \eta E} B_1(T_g)[1 - e^{-\tau_1}] + J_1\right] + K_1 t_l t_d I_1(0) e^{-\tau_1} \tag{12a}$$

$$M_2 = K_1 t_d\left[\frac{\alpha_1 + z\eta}{\alpha_1 + \eta E} B_1(T_g)[1 - e^{-\tau_1}] + J_1\right] \tag{12b}$$

$$M_3 = K_1 I_1(0) \tag{12c}$$

Solving for the measured blackbody ratios and optical depths allows for inspection of the introduced error

$$\Phi_1^m = \Phi_1 t_d(1 - e^{-\tau_1})/(1 - T_l t_d e^{-\tau_1}) \tag{13}$$

$$\tau_1^m = \tau_1 - \ln(t_l t_d) \tag{14}$$

$$\Phi_{1,2}^m = (\tau_1^m\Phi_1^m - \tau_2^m\Phi_2^m)/(\tau_1^m - \tau_2^m) \tag{15}$$

Temperature Measurements

The window transmissivities t_d and t_l will vary individually from one down to zero as the window fouls becoming opaque, so as one or both of the windows foul, the optical depth will increase and the single wavelength blackbody ratio will decrease. For the one wavelength measurement of temperature, fouling of the detector-side and lamp-side windows will cause additive errors. The error is greater for a transmission loss of the detector-side window but either gives a measured gas temperature that undervalues the true gas temperature, as shown in Fig. 3 for optical depths of $\tau_1 = 0.8$ and $\tau_2 = 0.2$.

In contrast, the errors are in opposite directions for the two-wavelength method; the two-wavelength blackbody ratio will overvalue the gas temperature if the lamp-side window fouls, and undervalue the temperature with fouling of the detector-side window. If both windows are fouled, the error for the two-wavelength technique lies somewhere between the two extremes shown in Fig. 3. In the fortuitous case of both windows fouling equally, the two-wavelength calculation of temperature remains reasonably well behaved down to 20% transmission; that is, only 45% transmission through each window for these optical depths. The single wavelength technique shows significant error, even at small transmission losses.

Observations by this author over several years indicate that the most severe window fouling occurs during the combustor

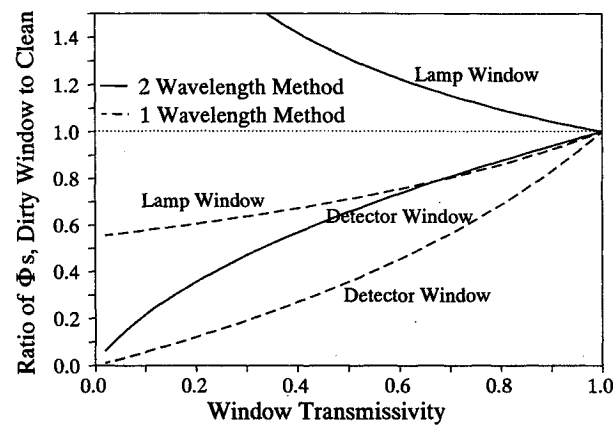

Fig. 3 Example bias in the Planck blackbody ratios for emission absorption measurements as a function of lamp- and detector-side window fouling.

ignition. If the optical ports can be shuttered during these time periods, the fouling of windows is minimal. If the windows cannot be shuttered and the fouling occurs during the ignition, then simply recording posttest the effective blackbody lamp temperature through the fouled lamp-side window and the lamp signal through both fouled windows and using these in the calculations will essentially eliminate the error in either measurement method. This presumes that transmission is not reduced in such a way as to reduce seriously the signal-to-noise ratio. The advantage of the two-wavelength method arises when the fouling occurs throughout the test. In this case, the systematic error from the indeterminate transmission losses is reduced by using the two-wavelength method. A limit can be placed on the error by measuring the posttest window transmissivities.

Figure 3 illustrates the effect of window fouling for the optical depths that are typically of measurements made in the laboratory or in small-scale combustion flows, $L \leq 20$ cm. Measurements made on coal-fired flows with heavy ash carryover and or with longer path lengths give significantly larger continuum optical depths, so that error from a fouled lamp window is reduced for the one-wavelength method. However, it is such particle-laden conditions that cause considerable error in the single wavelength temperature and number density measurements and make the two-wavelength methods preferable.

Emitter Number Density Measurements

The increase in the measured optical depth with window fouling will directly introduce error in the single wavelength measurement of emitter number density; this technique requires an absolute measure of optical depth at a particular wavelength on the resonance line. In contrast, the two-wavelength method will cancel the error in the optical depth, leaving only the error that arises in the temperature measurement, and even this bias is reduced by the square root relationship for a Voigt model. As long as there is some lamp light transmitted across the flow, window fouling will not introduce bias into the two-wavelength measurement of emitter atom number density.

Fluctuating Optical Misalignment

Emission absorption measurements require collection of a transmitted lamp signal eliminating light collection from any section of the flame that has not been transilluminated by the lamp. Problems in maintaining an optical alignment over long path lengths and on sometimes severely vibrating facilities can be considerable. On large-scale combustion facilities, slowly varying shifts in alignment will have an insignificant effect on the emission signal, but potentially will cause a loss of transmitted lamp signal affecting the emission absorption measurements in just the same way as lamp-side window fouling does. Careful selection of the optical elements and mounts can reduce this problem, and if access to the optics is available during testing, such shifts can be corrected for as they occur. However, the problem of rapidly fluctuating misalignment of the lamp image seems to have arisen in this test and presented here is an analysis of how such a misalignment biases the emission absorption measurements. If lamp misalignment occurs through beam steering caused by rapid pressure fluctuations in the flow or by vibration of the optical mounts, then a harmonic oscillator description for the misalignment between the lamp image and collection optics may be an appropriate model for analysis of the problem. Such a model is presented here to explain the test results and is referred to as a harmonic misalignment.

The analysis here is specific for the optical elements of this instrument but the treatment could easily be generalized to other optical geometries. A tungsten lamp with a 2-mm-wide strip filament is used as the reference lamp, and on the opposite side of the hot flow, a 1-mm core diameter optical fiber is used for light collection and transmission back to a monochromator and detector, in this case a vidicon detector. The fiber tip is carefully centered on the lamp image, leaving 0.5 mm of the lamp image on either side of the fiber tip for "grace"—this optical arrangement has been used successfully for many tests. Figure 4 shows how the effective lamp signal collection efficiency is reduced by displacement of the lamp image and also how the measured optical depth increases with the loss of the lamp signal.

Time-averaging over the harmonic displacement cycle reveals how the misalignment will affect measurements and Fig. 5 shows how the time-averaged lamp collection efficiency factor changes with vibration amplitude along with the standard deviation for a large sample of time-resolved measurements. Also shown is the average and standard deviation for the bias in the measured optical depth due to the vibration induced misalignment.

The instrument has a time resolution for illumination of the lamp and emission signals of about 0.25 ms with a separation of 0.5 ms so that knowledge of the misalignment frequency would be required to determine whether the results would be described as time-averaged or time-resolved. However, all of the spectral information for each signal is collected over the same time interval. If the detection system time-resolves the vibration, which seems to be indicated, then a large population of individual measurements of collection efficiency and optical depth bias would yield average and standard deviations, as shown in Fig. 5.

Time-Averaged Intensity Measurements

Writing the lamp collection efficiency factor as F, the time-averaged transmitted lamp signal can be written in terms of the average of F and its standard deviation (averages are

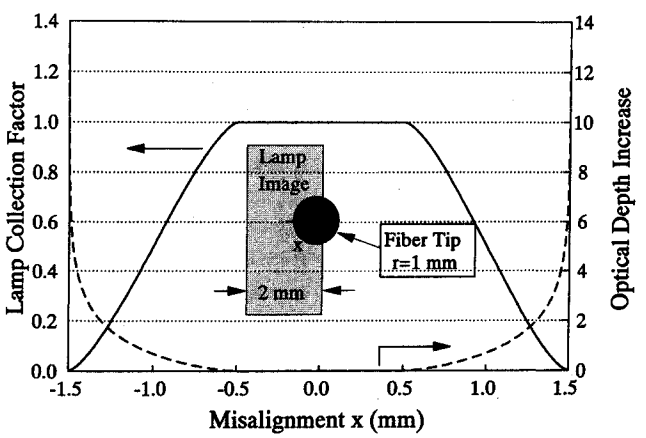

Fig. 4 Lamp collection efficiency factor and optical depth increase vs misalignment between a 1-mm-diam optical fiber and 2-mm-wide lamp filament image.

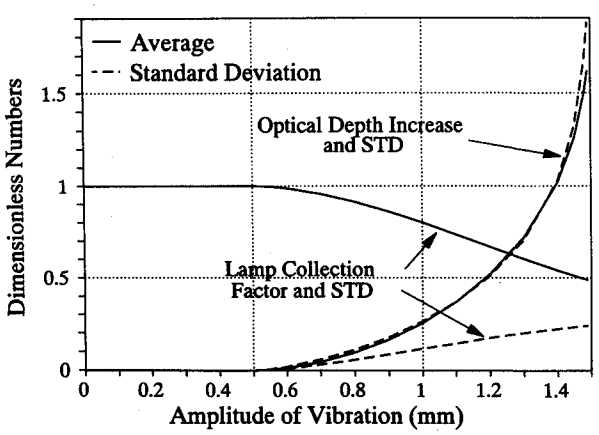

Fig. 5 Time-averages and standard deviations for lamp collection efficiency factor and optical depth increase vs harmonic amplitude of misalignment.

shown with overbars and standard deviations with δ)

$$\overline{M}_1 = K_1 \left[\frac{\alpha_1 + z\eta}{\alpha_1 + \eta E} B_1(T_g)[1 - e^{-\tau_1}] + J_1 + (\overline{F} \pm \delta F) I_1(0) e^{-\tau_1} \right] \quad (16)$$

and the expressions for measured optical depth and blackbody ratio can be written as

$$\tau_1^m = \tau_1 - \ln(\overline{F} \pm \delta F) \approx \tau_1 - \ln(\overline{F}) \pm \delta(F)/\overline{F}$$

$$(\text{If } \pm \delta F/\overline{F} << 1) \quad (17)$$

$$\Phi_1^m = \Phi_1(1 - e^{-\tau_1})/[1 - (\overline{F} \pm \delta F)e^{-\tau_1}] \quad (18)$$

Writing $\Phi_{1,2}^m$ in terms of these expressions allows for inspection of bias caused by the fluctuating misalignment in the two-wavelength calculation of temperature. The optical depths are overestimated and Φ_1 and Φ_2 are underestimated with greater error at smaller optical depths, so that the two-wavelength method overetimates the gas temperature as occurs with fouling of the lamp-side window.

The optical depth difference used in the number density calculation is

$$\tau_1^m - \tau_2^m = \tau_1 - \ln(\overline{F} \pm \delta F)_1 - \tau_2 + \ln(\overline{F} \pm \delta F)_2 \quad (19)$$

and will be reasonably accurate in spite of the oscillating misalignment if the transmitted lamp signals for the two-wavelengths are collected over the same time interval.

Average Time-Resolved Results

The average of a large set of time-resolved measurements are as follows for optical depth and blackbody ratio

$$\tau_1^m = \tau_1 - \overline{\ln(F)} \pm \delta[\ln(F)] \quad (20)$$

$$\Phi_1^m = \Phi_1(1 - e^{-\tau_1})\{\overline{1/(1 - Fe^{-\tau_1})} \pm \delta[1/(1 - Fe^{-\tau_1})]\} \quad (21)$$

These expressions also predict that the optical depths are overestimated and Φ_1 and Φ_2 are underestimated with greater error at smaller optical depths. Single wavelength measurements, then would underestimate the gas temperature and overestimate the emitter atom number density. In contrast, the two-wavelength $\Phi_{1,2}^m$ will measure high, as shown earlier for fouling of the lamp-side window.

The optical depth difference for the two-wavelength number density calculation is then

$$\tau_1^m - \tau_2^m = \tau_1 - \tau_2 \pm \delta[\ln(F)]_1 \pm \delta[\ln(F)]_2 \approx \tau_1 - \tau_2 \quad (22)$$

If the transmitted lamp signals for the two-wavelengths are collected over the same time interval, then the number density calculation will be accurate in spite of the oscillating misalignment and with no appreciable increase in uncertainty.

Experimental Results

Figure 6 plots as a function of time the optical depth at the on-line wavelength and the number of valid temperature calculations from a set of 50. When the magnet is energized, the optical depth decreases by about 0.6 and the number of valid measurements increases to typical numbers of 47–49. Both of these trends are consistent with a harmonic misalignment of the lamp beam that disappears with MHD operation of the channel. The preceding harmonic vibration analysis revealed

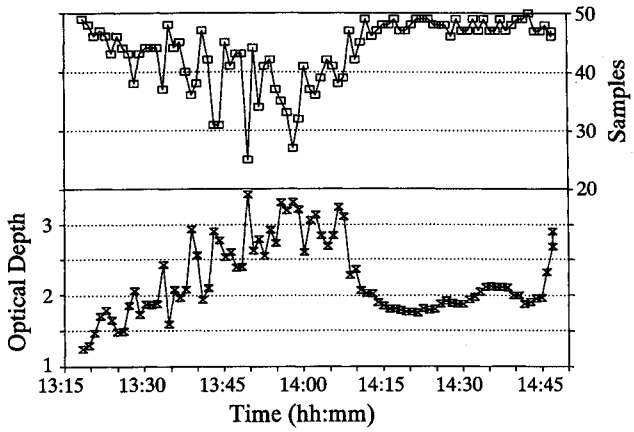

Fig. 6 On-line optical depth and statistical sample size for the average two-wavelength measurement of temperature vs time.

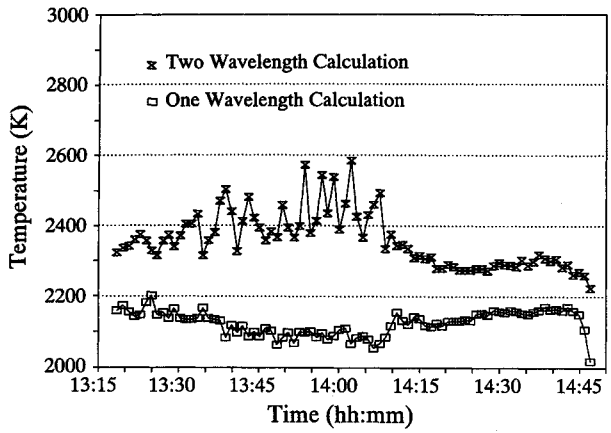

Fig. 7 Measured average temperatures vs time.

that the uncertainty in optical depth bias is nearly the same as the average bias. So if the bias is about 0.6, then the uncertainty is on the same order and many of the data sets would be invalid because the typical optical depth difference used for selection of wavelengths is 0.5. Some of the data sets before this time show low optical depths and large sample sizes indicating, perhaps, no misalignment problem and a good measure of the gas temperature prior to energizing the magnet.

Figure 7 shows the measurements of gas temperature vs time. If the bias is caused by misalignment, then the lowest averages recorded represent the best estimate of the true gas temperature. Indeed, reanalysis of the test data discarding data sets where the off-line lamp transmission is less than 10% yields temperatures around 2350 ± 50 K during this non-MHD portion of the test. After power extraction begins, the measured temperatures drop to around 2300 ± 30 K. A heat transfer calculation predicts a gas temperature of 2350 K at this location in the diffuser during the MHD power extraction.[16]

The optical depth after energizing the magnet is nearly as low as that observed at the beginning of the test, which suggests that there has been little fouling of the windows. The gradual climb in optical depth during MHD operation seems to be associated with an increase in potassium number density as argued below. At the end of the measurement span, the sudden increase in optical depth associated with a drop in samples indicates windows fouling.

Figure 8 shows temperature vs measured off-line optical depth for the MHD portion of the test. Looking first at optical depths below 2.2, temperatures calculated with the one-wavelength method show a 50 K drop as the optical depth varies from 2.1 to 1.7. This trend is consistent with error introduced by the particle emission, absorption, and scattering effects

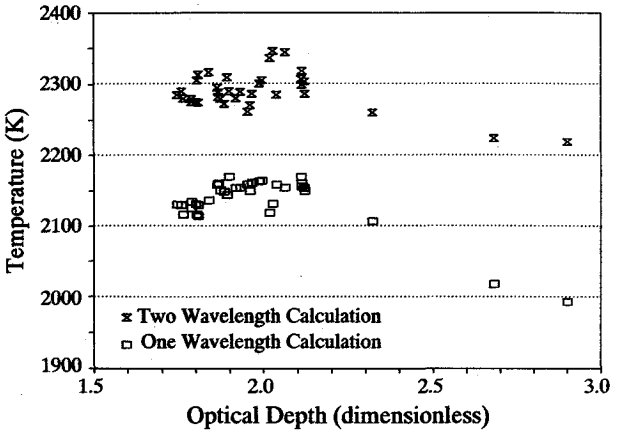

Fig. 8 Measured average temperatures vs on-line optical depth during MHD power extraction.

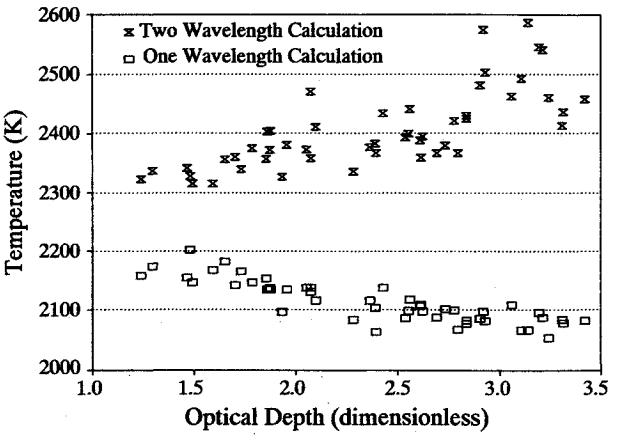

Fig. 9 Measured average temperatures, one- and two-wavelength calculations, vs on-line optical depth during non-MHD conditions.

that cause the one-wavelength method to underestimate the gas temperature with greater error at lower optical depth. Avoiding this bias is the reason for using the two-wavelength method on particle laden flows. The two-wavelength results show greater spread corresponding to an increased measurement uncertainty but are independent of optical depth as expected. From this plot, it is apparent that window fouling has not occurred before the last three data sets and, therefore, the trends observed with the two-wavelength temperature and number density measurements reflect true changes in the flow. While the trends in the single wavelength results also include particle bias and, thus, are more difficult to interpret, the emitter number density increase during this time span causes the one-wavelength method to over predict the temperature rise.

Measured optical depths greater than 2.2 all occur at the end of the measurement span and are consistent with the window fouling analysis presented in this article. At the greatest optical depth, which is for the last recorded measurement, the one-wavelength temperature has dropped by over 150 K nearly twice that for the two-wavelength calculation. This is consistent with fouling of the detector-side window.

Addressing the anomalous temperature fluctuations before power extraction, Fig. 9 plots the measured temperatures as a function of the off-line optical depth for the non-MHD portion of the test. The data sets for optical depths of 1.5 and below are measurements at the start of the test and seem unaffected by lamp misalignment. For the remaining sets, the single wavelength temperature results show a decrease of about 100 K in temperature with an increase in optical depth of about 2.0. The measured two-wavelength temperatures show an increased uncertainty with the higher optical depths and a trend toward higher temperatures. The temperature increase is at least 200 K; however, the sets with high measured optical depths correspond to small sample sizes, so the trend in temperature is difficult to quantify. These general trends are consistent though with a fluctuating lamp misalignment, a consequent bias in the measured optical depths and temperatures, and indicate a fairly large vibration amplitude.

Figure 10 shows the calculated potassium atom mole fraction for the one- and two-wavelength diagnostic methods. The consistent offset between the two results is the bias introduced into the single wavelength measurements by particle cloud absorption, leading to an overestimation in mole fraction of about 0.004. For the period before energizing the magnet, the single wavelength results are predicted by the harmonic misalignment analysis to be even higher because of the bias in the optical depth and this is reflected in the large mole fraction that drops as the magnet is energized. Indeed, the lack of appreciable change in the standard deviation of the two-wavelength atomic density, as shown in Fig. 2, is consistent with time-resolving the fluctuating misalignment.

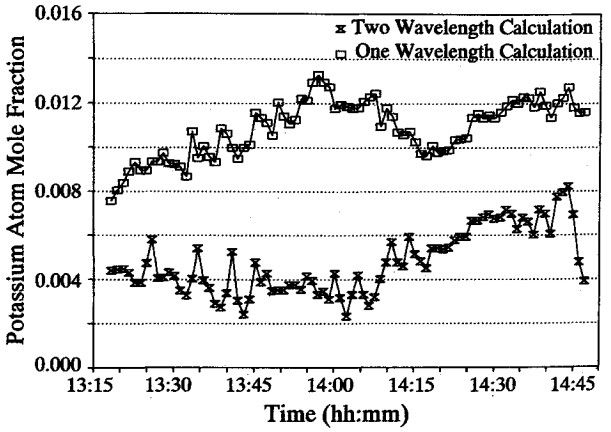

Fig. 10 Measured average potassium number density vs time.

At the end of the measurement period, as the windows are fouling, the one-wavelength calculation of density is near constant, while the two-wavelength measurement shows a steep decrease. This is consistent with bias in the one-wavelength method offsetting a true decrease in the atomic density, as shown by the two-wavelength results. The drop in seed density begins in advance of the log note stating that the seed flow was in manual mode and the later note that the seed flow was steadily dropping. It is not inconceivable that changes in control of the facility that lead to manual seed control were what caused the fouling of the windows.

In contrast and based upon the analysis presented in this paper, the trends in the two-wavelength calculations should be real since the method is unaffected by either problem because the measurement technique depends upon differences in optical depth cancelling out window transmissivity and misalignment induced biases. The results show a near steady value at a mole fraction of 0.004 that gradually doubles during the MHD generator operation before dropping at the end of the measurement period. Chemical equilibrium calculations predict a mole fraction of 0.0043 at a temperature of 2350 K for recorded test conditions at a time of 14:40 during generator operation, while at that time emission absorption measurements yielded a potassium mole fraction of 0.0067 ± 0.0017 and a temperature of 2295 ± 31 K.

Conclusions

The anomalous two-wavelength temperature measurements on this test have been explained by a rapidly fluctuating misalignment of the lamp image on the collection optics. A harmonic oscillator model was used to analyze the bias and uncertainty that arises from such a misalignment, although the source of the misalignment has not been identified. The

very large temperature uncertainty in the two-wavelength method arises because of the form of the equation that depends upon the difference in optical depths at the two wavelengths. The one-wavelength method suffers bias but not the dramatically increased uncertainty. The one-wavelength method could be considered preferable because of the smaller uncertainty, but using such a method there would have been no indication of the misalignment problem—the observed lower temperatures and higher densities would have been presumed to be real.

Also presented was an analysis of the bias introduced by window fouling into the temperature and number density methods. The analysis reveals that the observed drop in potassium number density at the end of the measurement period is real. The misalignment fluctuations do not affect the two-wavelength measurement of number density and the measured variations in number density for the test are presumably valid.

On particle-laden combustion flows where window fouling is a problem or on large-scale systems where vibrations and long pathlengths exacerbate alignment problems, two-wavelength, time-resolved emission absorption techniques can provide accurate diagnostic measurements of atomic density. Such line-of-sight measurements, because of their low-cost, reliable instrumentation and simple analysis, can provide robust monitoring of large-scale combustion flows.

Acknowledgments

This work was supported by the U.S. Department of Energy Contract DE-AC02-80ET15601. I thank Mike McCarthy for support of the Potassium Emission Absorption System in the field measurements, John Luthe for restoring the test data for reanalysis, and R. Arunkumar for heat transfer/chemical equilibrium calculations.

References

[1]Bauman, L. E., and Wolverton, M. K., "Time Resolved Line Reversal Gas Temperature Measurements using a Multi-Channel Detector," *Ninth International Conference on Magnetohydrodynamic Electrical Power Generation,* Vol. 2, 1986, Tsukuba, Ibaraki, Japan, pp. 563–572.

[2]Self, S. A., and Kruger, C. H., "Diagnostic Methods in Combustion MHD Flows," *Journal of Energy,* Vol. 1, No. 1, 1977, pp. 25–43.

[3]Bauman, L. E., "Gas Temperature Measurements of Particle-Laden MHD Flows," *Proceedings of the 22nd Symposium on Engineering Aspects of MHD,* Starkville, MS, 1984, pp. 8:3:1–3:17.

[4]Daily, J. W., and Kruger, C. H., "Effects of Cold Boundary Layers on Spectroscopic Temperature Measurements in Combustion Gas Flows," *Journal of Quantitative Spectroscopy and Radiation Transfer,* Vol. 17, No. 3, 1977, pp. 327–338.

[5]Onda, K., Kaga, Y., and Kato, K., "Measurement of MHD Combustion-Gas Temperatures and Potassium Number Densities in the Presence of Cold Boundary Layers," *Journal of Quantitative Spectroscopy and Radiative Transfer,* Vol. 26, No. 2, 1981, pp. 147–156.

[6]Bauman, L. E., Luthe, J. C., and Ma, X., "An Emission Absorption Technique Suitable for Automatic Measurement of Seed Atom Density in Coal-Fired MHD Flows," *Proceedings of the 27th Symposium of Engineering Aspects of MHD,* Reno, NV, 1989, pp. 8:3:1–8:3:6; see also *MHD: An International Journal* (submitted for publication).

[7]Paul, P. H., and Self, S. A., "Method for Spectroradiometric Temperature Measurements in Two Phase Flows. 1: Theory," *Applied Optics,* Vol. 28, No. 11, 1989, pp. 2143–2155.

[8]Daily, J. W., "Effect of Turbulence on Line-Reversal Temperature Measurements," *Journal of Quantitative Spectroscopy and Radiative Transfer,* Vol. 17, No. 3, 1977, pp. 339–341.

[9]Kowalik, R. M., "Measurements of Conductivity Nonuniformities and Fluctuations in Combustion MHD Plasmas," High Temperature Gas Dynamics Lab., Stanford Univ., Stanford, CA, No. 114, 1980.

[10]Stepan, I. E., Hart, A. T., Rivers, T. J., and Glovan, R. J., "Coal-Fired MHD Test Progress at the Component Development and Integration Facility," *Proceedings of the 28th Symposium on Engineering Aspects of MHD,* Chicago, IL, 1990, pp. I.1.1–12.

[11]Lindgard, A., and Nielsen, S. E., "Transitions Probabilities for the Alkali Isoelectronic Sequences," *Atomic Data and Nuclear Data Tables,* Vol. 19, No. 2, 1977, pp. 533–633.

[12]Hinnov, E., and Kohn, H., "Optical Cross Sections from Intensity-Density Measurement," *Journal of the Optical Society of America,* Vol. 47, No. 1, 1957, pp. 156–162.

[13]Self, S. A, Vasileva, I. A., and Nefedov, N. P., "Plasma Diagnostics in an MHD Installation," *Open Cycle Magnetohydrodynamic Electrical Power Generation*, edited by M. Petrick and B. Ya. Shumyatsky, U.S. Dept. of Energy, Argonne National Lab., Argonne, IL, 1978, pp. 637–644.

[14]Goodwin, D. G., and Mitchner, M., "Lineshape Measurements of Potassium for Radiation Heat transfer in MHD Generators," *Proceedings of the 20th Symposium on Engineering Aspects of MHD,* Irvine, CA, 1982, pp. 8.4.1–5.

[15]Bauman, L. E., "Potassium D-Line 'Blue' Wing Absorption Coefficient Under Combustion-Fired MHD Conditions," AIAA Paper 91-1513, Seattle, WA, June 1991.

[16]Private communication with Mr. Arunkumar, Research Engineer, Diagnostic Instrumentation and Analysis Lab., Mississippi State Univ.